Differential roles of STAT1 α and STAT1 β in fludarabine-induced cell cycle arrest and apoptosis in human B cells

Fanny Baran-Marszak, Jean Feuillard, Imen Najjar, Christophe Le Clorennec, Jean-Marie Béchet, Isabelle Dusanter-Fourt, Georg W. Bornkamm, Martine Raphaël, and Remi Fagard

Signal transducer and activator of transcription 1 (STAT1), a transcription factor known to participate in antiviral responses, acts as a tumor suppressor inhibiting cell growth and promoting apoptosis. To study the role of STAT1 in DNA damage-induced apoptosis in B lymphocytes, its active form, STAT1 α , was specifically inhibited by the overexpression of STAT1 β , the STAT1 α truncated inhibitory isoform. An episomal vector with a tetracycline-inducible bidirectional promoter was created to induce the expression of 2 proteins, STAT1ß and enhanced green fluorescence protein (EGFP). The same vector was used to overexpress STAT1 α

as a control. Expression of STAT1ß inhibited the phosphorylation, the DNA-binding activity, and the transcriptional activity of STAT1 α , as well as the expression of STAT1α target genes such as p21WAF1/ CIP1, TAP1, IRF1, and PKR. Inhibiting STAT1 α by STAT1 β increased the growth rate of transfected cells and their resistance to fludarabine-induced apoptosis and cell cycle arrest. Overexpressing STAT1ß reversed the negative regulation of Mdm2 expression observed after treatment with interferon-gamma (IFN-γ), which activates STAT1, or with fludarabine. Nuclear translocation of p53 after fludarabine treatment was decreased

when STAT1 β was overexpressed, and it was increased when STAT1 α was induced. Oligonucleotide pull-down experiments showed a physical STAT1/p53 interaction. Our results show that imbalance between the antiproliferative/proapoptotic isoform STAT1 α and the proliferative isoform STAT1 β is likely to play a crucial role in the regulation of proliferation and apoptosis and that STAT1 α may regulate p53 activity and sensitize B cells to fludarabine-induced apoptosis. (Blood. 2004;104:2475-2483)

© 2004 by The American Society of Hematology

Introduction

Initially identified by their activation in response to interferon (IFN),¹⁻⁴ the STATs (signal transducers and activators of transcription) are a family of 7 latent cytoplasmic proteins that regulate the expression of numerous genes involved in several cell functions, among them immune response, protection against viral infection, cell proliferation, differentiation, and apoptosis.⁵⁻¹³ Many receptors for cytokines, growth factors, and hormones activate the family of Janus kinases (Jaks) or other tyrosine kinases, which, in turn, phosphorylate the STATs. Once phosphorylated, the STATs form homodimers or heterodimers that translocate from the cytoplasm to the nucleus and bind to a palindromic DNA motif in the regulatory region of STAT-regulated genes.^{3,14} Recently, this model was challenged by the demonstration of a shuttle of STAT3 taking place in the absence of activation.¹⁵

Type 1 and type 2 IFNs activate STAT1.¹⁶ STAT1 contains a carboxy terminal transcription activation domain (TAD), which is required for maximal transcriptional activation.¹⁷⁻¹⁹ Alternative splicing generates 2 naturally occurring forms of STAT1: STAT1 α (91 kDa) and STAT1 β (84 kDa).²⁰ The β form lacks the 38 residues

encompassing the TAD and has been found to be transcriptionally inactive. 4,20,21 In addition, the deletion of TAD exerts a dominant-negative action on STAT1 α . 22 IFN- γ induces the formation of homodimeric STAT1, and STAT1 is implicated in the inhibition of cell proliferation in several cell systems 23,24 and can act as a tumor suppressor in many cell types by inducing the expression of cyclin kinase inhibitors and caspases in response to extracellular stimuli. 6,7,13,25,26 IFN- γ can also activate signaling pathways and transcriptional programs that promote or inhibit cell proliferation. 27

The chemotherapeutic agent fludarabine is widely used to treat B-cell malignancies, including B-cell chronic lymphocytic leukemia (B-CLL), mantle cell lymphoma, and Waldenstrom macroglobulinemia.²⁸ This adenosine nucleoside analog induces cell cycle arrest and apoptosis and is thought to act primarily through the activation of p53. Fludarabine also appears to be related to STAT1: its cytotoxicity is associated with a specific depletion of STAT1 in B-CLL cells,²⁹ and it was found to be inefficient in killing in vitro Epstein-Barr virus (EBV)–infected B cells that exhibit constitutive activation of STAT1 or EBV-converted STAT1-expressing Burkitt

From the Equipe d'Accueil 3406 Université Paris 13, Service de Biochimie, Hôpital Avicenne, France; Unité Mixte de Recherche (UMR) Centre National de la Recherche Scientifique (CNRS) 6101 and Laboratoire d'Hématologie, Centre Hospitalier Universitaire (CHU) Dupuytren and Faculté de Médecine, Université de Limoges, France; Institut National de la Santé et de la Recherche Médicale (INSERM) E109, Université Paris 11, Kremlin-Bicêtre, France; UMR 6551, Université de Caen, France; Unité INSERM Institut Cochin de Génétique Moléculaire (ICGM) Cochin Port-Royal, France; and Forschungszentrum für Umwelt und Gesundheit (GSF)—Institute of Clinical Molecular Biology and Tumor Genetics, Munich, Germany.

Submitted October 15, 2003; accepted April 21, 2004. Prepublished online as *Blood* First Edition Paper, June 24, 2004; DOI 10.1182/blood-2003-10-3508.

Supported by Association de Recherche contre le Cancer grant 5861, the Ligue

contre le Cancer, Comité Ile de France, the Ligue Nationale contre le Cancer (labellisation Ligue 2002 UMR CNRS 6101), INSERM/DFG, and Fondation de France, and by grants from the Deutsche Forschungsgemeinschaft (DFG-SFB455) (G.W.B.), the Wilhelm-Sander-Foundation, and Ligue contre le Cancer, Comité de la Creuse (C.Le C.).

Reprints: Remi Fagard, EA 3406 Université Paris 13, Service de Biochimie, Hôpital Avicenne, 125 route de Stalingrad, 93009 Bobigny Cedex, France; e-mail: remi.fagard@avc.ap-hop-paris.fr.

The publication costs of this article were defrayed in part by page charge payment. Therefore, and solely to indicate this fact, this article is hereby marked "advertisement" in accordance with 18 U.S.C. section 1734.

© 2004 by The American Society of Hematology

lymphoma (BL) cell lines,³⁰ whereas it was able to kill their EBV-negative counterparts expressing very low levels of STAT1 protein. By contrast, B-CLL resistance to apoptosis is associated with decreased STAT1 expression.³¹ STAT1 has been shown to interact with p53.³² It has also been found to regulate TNF receptor associated death domain (TRADD)-dependent signaling, resulting in NF- κ B inhibition.³³ Most papers address only the role of STAT1 α , but STAT1 α and STAT1 β are likely to play different and eventually opposite roles.¹² The role of STAT1 in fludarabine-induced cell cytotoxicity certainly must be understood because some clinical studies have begun to evaluate the combination of chemotherapies that may include IFN plus fludarabine for the treatment of low-grade lymphomas.³⁴⁻³⁸

The aim of this work was to investigate the roles of STAT1 α and STAT1B in the inhibition of proliferation and the induction of apoptosis by fludarabine in B cells. We used a continuously proliferating EBV-immortalized lymphoblastoid cell line (LCL) in which STAT1 is constitutively activated.^{30,39} To inhibit the active form of STAT1α, we overexpressed STAT1β. To monitor the overexpression of STAT1B, we constructed a new episomal tetracycline-inducible vector that allows coexpression of the cDNA of interest (in this case, STAT1B) and the enhanced green fluorescence protein (EGFP) as a marker of induction. We found that inhibiting STAT1 α was associated with decreased expression of several STAT1 target genes, including the CDK inhibitor p21WAF1, and with resistance to fludarabine-induced cell cycle arrest and apoptosis, resulting in an increased rate of cell proliferation. Finally, we observed a reversal of the fludarabine-induced inhibition of expression of Mdm2 by STAT1B, which, together with the interaction we observed of STAT1α with p53, might explain in part the STAT1\(\beta\)-induced resistance to apoptosis.

Thus, fludarabine-induced cell cycle arrest and apoptosis are dependent on STAT1 α , and the closely regulated STAT1 α /STAT1 β balance itself may play a role in the resistance of B lymphocytes to this cytotoxic agent.

Materials and methods

Plasmid constructs

The CKR516 vector is schematically depicted in Figure 1. The CKR516 backbone is derived from the MS4A vector. 40 The cassette encoding the reverse tetracycline repressor-transactivator fusion protein (rtTA) was replaced by the one encoding the improved rtTA2s-M2 protein.⁴¹ To avoid NF-κB interference in the expression of rtTA2^s-M2, the cytomegalovirus (CMV) promoter driving the expression of the tetracycline-regulated transcription factor that contains 4 NF-kB binding sites, was replaced by a composite Eμ-RSV promoter without any NF-κB site. The Eμ-RSV composite promoter harbors the Rous sarcoma virus promoter and an AatII-EcoRI fragment encompassing the mouse Eμ intron enhancer.42 The tetracycline-responsive modified tetO7/EBV-LMP2A promoter was replaced by the AatII-HindIII fragment of the pBI-EGFP plasmid containing both the bidirectional tetracycline-responsive promoter with the heptamerized tet operator sequences and the cassette encoding the optimized EGFP.^{43,44} An AscI site was inserted between EGFP and the ampicillin resistance gene, and a NotI site was inserted between rtTA2s-M2 and oriP to facilitate further cloning steps. STAT1 α and STAT1 β cDNAs were excised as NotI-ApaI fragments of the RcCMV plasmid, 20,45 made blunt ended, and, after ligation of an SfiI linker, subcloned into the SfiI sites of the CKR 516 vector.

Cell culture, transfections, and functional promoter analysis

The lymphoblastoid cell line PRI was cultured in RPMI 1640 (Eurobio, Les Ulis, France) supplemented with 10% decomplemented fetal calf serum

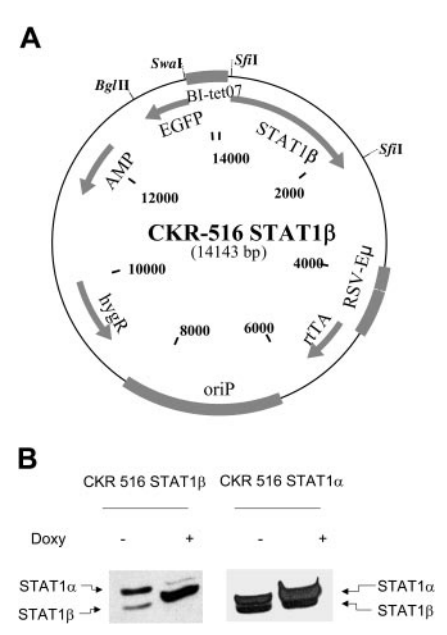


Figure 1. Induction of STAT1β and STAT1α. (A) Schematic diagram of the CKR516-STAT1β vector. Gray boxes indicate cassettes; BI-tet07, bidirectional tetracycline-responsive promoter; STAT1β, cDNA encoding STAT1β; EGFP, cDNA encoding the enhanced green fluorescence protein; rtTA, reverse tetracycline-repressor transactivator fusion protein rtTA2s-M2; EBV oriP, origin of replication of the EBV plasmid; HygR, gene for hygromycin resistance; E_{μ} -RSV, promoter-enhancer consisting of mouse immunoglobulin heavy chain intron enhancer and RSV promoter; and Sfl, restriction sites for Sfl. (B) Expression of STAT1β and STAT1α in LCL cells transfected with CKR516-STAT1β and CKR516-STAT1α. STAT1β and STAT1α expression was assessed after 4 weeks of selection by hygromycin using Western blotting with an anti-STAT1 antibody recognizing STAT1α (91 kDa) and STAT1β (84 kDa), as indicated by arrows. Analysis was performed in transfected cells that were either treated (+) or not treated (-) with 1.5 μg/mL doxycycline for 24 hours. This experiment is representative of 4 independent transfections of cells. In each case, the percentage of EGFP-inducible cells was approximately 70%.

(Dutcher, Brumath, France), 100 U/mL penicillin, 10 μ g/mL streptomycin (GibcoBRL, Life Technologies, Cergy Pontoise, France), and 2 mM L-glutamine (Eurobio) at 37°C in a humidified 5% CO₂ atmosphere. Transfections, selection of hygromycin-resistant cells, and doxycycline treatment were performed as described. GGFP inducibility and STAT1 β or STAT1 α expression were assessed by flow cytometry and Western blotting, respectively, after 6 weeks of hygromycin selection. Where indicated, cells were treated with 250 U/mL IFN- γ (Roche Diagnostics, Meylan, France) for 30 minutes or 24 hours or with 15 μ M fludarabine for 24 hours.

Functional promoter analysis was performed by cotransfecting the STAT1 β – or STAT1 α –transfected cells with a TAP1 promoter reporter luciferase construct with an inactivated κB site (a generous gift of Dr D. Johnson). Cells were lysed with 200 μL lysis solution (Tropix kit; Applied Biosystems, Foster City, CA) supplemented with 1 mM dithiothreitol (DTT) for 15 minutes. One hundred microliters luciferase substrate A (Tropix) and 100 μL luciferase substrate B (Tropix) were added to 20 μL cellular lysate. The luciferase was quantitated on a luminometer (BCL Book Luminometer; Promega, Madison, WI).

Western blotting

Cells were counted using an Advia 120* apparatus (Bayer Diagnostic, Puteaux, France). Total protein extracts were obtained as follows: 5 million cells were resuspended in 100 μL lysis buffer containing 0.01% bromophenol blue (Bio-Rad, Hercules, CA), 50 mM Tris HCl, pH 6.8, 2% sodium dodecyl sulfate (SDS), 20% glycerol (Sigma, St Louis, MO), and 5% 2-mercaptoethanol (Bio-Rad). Lysates were sonicated and stored at $-80^{\circ} C$. Twenty microliters boiled extracts (1 million cells) were resolved on a 10% polyacrylamide denaturing gel at 300 V for 3 hours and were electrophoretically transferred (Hoefer Scientific Instruments, San Francisco, CA) on a nylon (Immobilon; Millipore, Bedford, MA) or nitrocellulose (Schleicher

& Schuell, Dassel, Germany) membrane. Membranes were stained with Ponceau red to check that equal amounts of protein were present in each lane. After blocking the membranes for 2 hours in 3% dry skim milk in Tris-buffered saline (TBS; Bio-Rad) (20 mM NaCl, 500 mM Tris-HCl, pH 8), incubation with the first antibody was performed overnight in TBS containing 0.1% Tween 20 (Sigma) and 1% dry skim milk. Antibodies used were anti-STAT1 (rabbit polyclonal; Cell Signaling, Beverly, MA) at 1:500, antiphosphotyrosine-701 STAT1 (rabbit polyclonal; Cell Signaling) at 1:500, anti-myc-tag (9E10 mouse monoclonal; Santa Cruz Biotechnology, San Diego, CA) at 1:1000, anticleaved poly(ADP-ribose)polymerase (PARP) at 1:1000 (Cell Signaling), and antiactin at 1:1000 (Santa Cruz Biotechnology). After 60 minutes of washing in TBS 0.1% Tween, the corresponding horseradish peroxidase-conjugated secondary antibody (goat antimouse; Bio-Rad) at 1:5000, goat antirat (Santa Cruz Biotechnology) at 1:5000, or goat antirabbit (Bio-Rad) at 1:5000 was added for 45 minutes. Revelation was performed after washing for 2 hours in TBS 0.1% Tween, 1% dry milk, by enhanced chemiluminescence (ECL; Amersham, Orsay, France) and autoradiography (X-Omat-R films; Kodak, Rochester, NY).

Electrophoretic mobility shift assay and oligonucleotide pull-down assay

Nuclear and cytosolic proteins were extracted as described previously.⁴⁶ Ten micrograms nuclear protein extracts in 5 µL extraction buffer C (20 mM HEPES [N-2-hydroxyethylpiperazine-N'-2-ethanesulfonic acid], 25% glycerol, 0.5 M NaCl, and 1.5 mM MgCl₂) were mixed with 1 µL annealed ³²P-labeled m67-SIE DNA probe (sequence, 5'-CATTTCCCGTAATC-3') (Genset, Paris, France) in a solution containing 10 mM HEPES, pH 8, 100 μM EDTA (ethylenediaminetetraacetic acid), 0.05 M NaCl, 5 mM MgCl₂, 4 μM spermidine (Eurolab; Merck, Strasbourg, France), 2 mM DTT, 0.1 mg/mL bovine serum albumin (BSA), 2.5% glycerol, 4% Ficoll, and 2 μg poly(dI-dC) (Roche) (binding buffer) and were incubated for 30 minutes at room temperature. For supershift assays, preliminary incubation was performed with 1 μL anti-STAT1α antibody (mouse monoclonal c-111; Santa Cruz Biotechnology) or anti-STAT1α/β (H2 mouse monoclonal; Cell Signaling). DNA-protein complexes were separated on a 6% nondenaturing polyacrylamide gel in 0.25 × Tris-Borate-EDTA buffer (Bio-Rad) by 4-hour migration at 250 V. The gel was dried and exposed to a phosphor imaging screen (Packard Instruments, Meriden, CT). The radioactive signal was visualized using a phosphor system analyzer (Cyclone; Packard

Oligonucleotide pull-down assays were performed with an annealed nucleotide comprising the p53 consensus site (5'-GGACATGCCCGGGCATGTC-3') with a 5' biotin label. Nuclear extracts (50-100 μg) were incubated for 1 hour at 4°C with 1 μg oligonucleotide in binding buffer. Sepharose–streptavidin (50 μL ; Sigma) was added for 2 hours at 4°C. After 3 washes in a buffer containing 10 mM Tris-HCl, pH 8, 100 mM NaCl, and 1 mM EDTA, the complexes were resuspended in SDS sample buffer and were separated on 8% polyacrylamide SDS gels, transferred to nitrocellulose membranes (Schleicher & Schuell), and processed for Western blotting as described above using anti-STAT1 and anti-p53 antibodies (Cell Signaling).

Flow cytometry analysis, cell sorting, and cell proliferation measurement

Induction of EGFP expression was assessed by flow cytometry. Cells were washed in phosphate-buffered saline (PBS; BioMérieux, Marcy l'Etoile, France) and resuspended in 1 mL PBS containing 2 $\mu g/mL$ propidium iodide (PI; Sigma). EGFP-positive cells were counted within the population of viable (PI-negative) cells using the FL1 photomultiplier of either an XL Beckman/Coulter or a FACSCalibur flow cytometer. Where indicated, EGFP-positive and EGFP-negative cells were sorted using a FACSVantage cell sorter.

Determining the fraction of cells in S phase was performed as described. 40 Cells were washed, resuspended in 300 μL PBS, and fixed in 70% ethanol at $-20^{\circ}C$ for 24 hours. Cells were further processed by

incubation in 1 mL HCl 2 N, 0.2 mg/mL pepsin for 30 minutes at room temperature, followed by neutralization with 3 mL Na₂B₄O₇. Then cells were washed in PBS, resuspended in PBS containing 0.1% Triton X100 (Sigma) (PBS-Triton), and incubated with 5 μ L anti-bromodeoxyuridine–fluorescein isothiocyanate (anti-BrdU-FITC; PharMingen, San Diego, CA) for 30 minutes. Cells were then washed in PBS-Triton and incubated for 30 minutes at room temperature in 0.5 mL PBS-Triton containing 0.1 mg/mL RNase (Sigma) and 10 μ M PI (Sigma) before analysis by flow cytometry.

To measure cell proliferation, the cells were washed and resuspended at a density of $7\times10^5/mL$ in a final volume of 3 mL culture medium. Cells were counted every day for 4 days from a $300\text{-}\mu\text{L}$ aliquot using an Advia 120^* cell counter. Cell number was adjusted to $10^6/mL$ by adding culture medium. The total number of cells was then calculated. Doubling time was calculated by analysis of the kinetics of cell proliferation once the exponential proliferation phase had been reached.

Real-time quantitative polymerase chain reaction

Total RNA was extracted from purified transfected EGFP-positive and -negative cells using the Qiagen kit following the recommendations of the manufacturer. We defined, as a reference RNA, a pool of RNAs (RNA pool) extracted from 5 different tonsils, lymph nodes, and spleens with benign reactive follicular hyperplasia.

RNA levels for *p21*, *IRF1*, *TAP1*, and *PKR* genes were quantified in parallel in the different RNA extracts and in the RNA pool on an ABI PRISM 7000 Automat using the TaqMan Assay-on-Demand gene expression products reference system (Applied Biosystems) corresponding to the reference products Hs00355782_m1, HS00233698_m1, HS00388682_m1, and HS00169345_m1, respectively. *Abl1* gene was used as a reference gene for control of amplification (reference HS00245443_m1). Reverse transcription was performed with 2 µg total RNA with the Archive kit RT from Applied Biosystems in a final volume of 50 µL. Gene amplification was performed with 1.25 µL cDNA, corresponding to 50 ng total RNA. All these steps were performed following the recommendations of the manufacturer.

Relative expression levels of each gene were calculated as already reported. ⁴⁷ Briefly, for each gene, the cycle threshold (CT) was defined for a δ Rn of 10^{-1} . Then, the δ CT (DCT) was calculated as the CT of the gene minus the CT of Abl1 (expected CT for Abl1 range, 22-24). For each given experimental condition, the $\delta\delta$ CT (DDCT) was calculated as the DCT of the given condition minus the DCT of the RNA pool. For each gene and in each given experimental condition, the calculated relative gene expression level was equal to 2^{-DDCT} .

Immunofluorescence

P53 detection by immunofluorescence was performed on cytocentrifuged cells (50 000 cells/slide) by incubating the D07 monoclonal antibody (DAKO, Carpinteria, CA) diluted at 1:50. Biotinylated antimouse immune serum from the LSAB kit (DAKO) was used undiluted as a second step of the revelation. For the third step, AlexaFluor 594 streptavidin was used (Molecular Probes, Leiden, The Netherlands) and was diluted at 1:100. Each labeling step was performed in PBS containing 1% fetal calf serum (FCS) for 30 minutes and was followed by 2 washes in PBS. Counterstaining of nuclei was done with DAPI diluted at 0.05 mg/mL. Slides were mounted in DABCO medium (Sigma) diluted at 2.5% in a solution containing 90% glycerol and 10% PBS. Three-color (EGFP, AlexaFluor 594, DAPI) fluorescence signals were acquired, and electronic capturing and merging of the 3 pictures was performed on a Visys station. Controls were performed in parallel using an irrelevant mouse monoclonal antibody and showed no significant background (not shown).

Used in Figure 7C were a Zeiss Axiophot (first panel), Plan Neofluar $100 \times /1.30$ (second panel), Alexa Fluor 536/EGFP/DAPI (third panel), Photometrics SenSys camera (fourth panel), QUIPS (fifth panel), and nothing for the sixth panel.

Results

Coinduction of STAT1 β or STAT1 α and EGFP

To specifically inhibit the transcriptional activity of STAT1 α , we overexpressed STAT1 β using a tetracycline-inducible vector. As a control, we used the same vector to induce STAT1 α overexpression. The vector contained a bidirectional promoter⁴⁸ that was positively regulated by doxycycline, promoting simultaneously the expression of 2 independent cDNAs coding for the EGFP as a marker of induction and for STAT1 β (Figure 1A) or STAT1 α .

After transfection, the cells were grown in selection medium for 6 weeks. After adding doxycycline, coinducibility of EGFP and STAT1β or STAT1α was analyzed using flow cytometry and Western blotting (Figure 1B). Preliminary experiments determined that a plateau of EGFP induction was reached at a concentration of 0.6 µg/mL doxycycline (not shown). A minor background of EGFP expression was detected in the absence of the inducer (Figure 2A), indicating either a higher autofluorescence of cells after transfection or that tetracycline regulation in this system is slightly leaky. A dose-response experiment with doxycycline concentrations ranging from 0 to 0.6 µg/mL, applied for 24 hours, showed that STAT1 β or STAT1 α induction was parallel to EGFP induction (Figure 2B and not shown). Moreover, analysis of the kinetics of EGFP and STAT1β or STAT1α induction revealed that increased expression of EGFP was detectable after 4 hours of doxycycline treatment, reached a maximum after 24 hours, and was then stable for 4 days. Induction of STAT1 α or β always coincided with EGFP induction (not shown). Thus, this system of coexpression of a reporter gene such as EGFP allowed assessment of the proportion of induced cells and the level of gene induction in individual cells.

Overexpression of STAT1 β inhibits STAT1 α activation

To investigate the effect of STAT1 β overexpression on STAT1 α activity, we analyzed the phosphorylation of Tyr701 and the

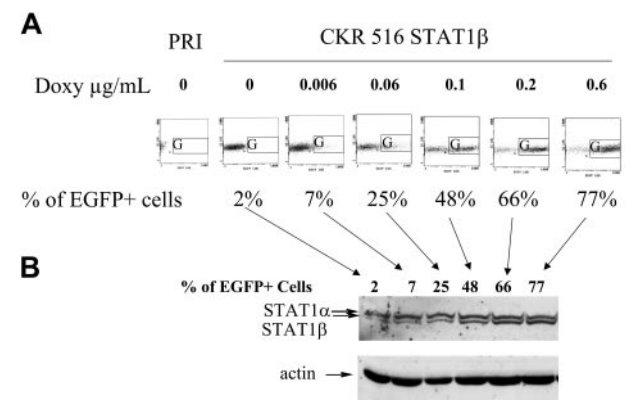
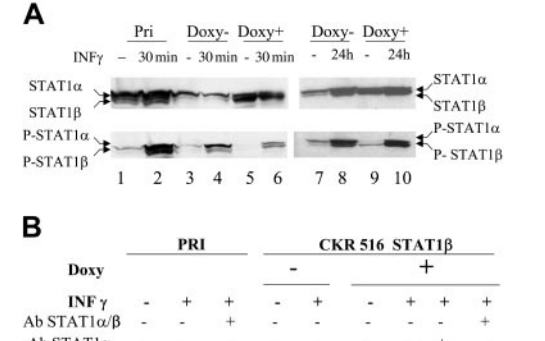


Figure 2. Comparison between EGFP and STAT1β induction. (A) Dose-response induction of EGFP. The expression of EGFP was analyzed in nontransfected PRI cells (PRI) and in CKR516-STAT1β-transfected cells after 4 weeks of selection by hygromycin. Autofluorescence of nontransfected PRI cells was lower than that of CKR516-STAT1β-transfected cells and did not change with doxycycline treatment CKR516-STAT1β-transfected cells positive for EGFP after 24 hours of treatment with 0 to 0.6 μg/mL doxycycline were detected by flow cytometry in the G area on an FL1/side-scatter dot plot. The concentration of doxycycline is indicated above each graph. The percentage of EGFP-positive cells is indicated under each graph. (B) Dose-response induction of STAT1β. Western blot analysis was performed as for Figure 1. Analysis was performed in the same cells in panel A, with EGFP induction ranging from 2% to 77%. Arrows indicate the correspondence between the EGFP flow cytometry dot plot and the different lanes of the Western blot. Results are representative of 2 different experiments. Comparable results were obtained with CKR516STAT1α-transfected cells.



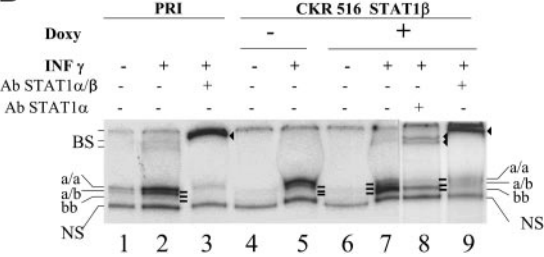


Figure 3. Inhibition of STAT1 α activity in STAT1 β overexpressing cells. (A) Expression and phosphorylation status of STAT1 α and STAT1 β . Phosphorylation status of STAT1\alpha and STAT1\beta was assessed using Western blotting with an antiphosphotyrosine 701 STAT1 antibody. Cells were treated (+) (lanes 5, 6, 9, and 10) or not treated (-) (lanes 3, 4, 7, and 8) with doxycycline for 24 hours. Parental (lanes 1 and 2) and transfected (lanes 3-6) PRI cells were treated (lanes 2, 4, 6, and 10) or not treated (lanes 1, 3, 5, 7, and 9) with IFN-ν (250 U/mL) for 30 minutes (lanes 2, 4, and 6) or for 24 hours (lanes 9 and 10). Note that lanes 3 and 7 and lanes 5 and 9 represent identical samples from 2 independent experiments. (B) Analysis of the binding activity of the STAT1 isoforms to the SIE DNA probe. The binding activity to SIE was assessed using EMSA with 10 μg nuclear protein extract from parental (lanes 1-3) and transfected (lanes 4-9) cells that were either treated (+) (lanes 5, 7, 8, and 9) or not treated (-) (lane 4) with doxycycline for 24 hours and either treated (+)(lanes 2, 3, 5, 7, 8, and 9) or left untreated (-) (lanes 1 and 4) with IFN- γ (250 U/mL). Nuclear extracts were obtained from the cells shown in panel A, lanes 1 to 6. Extracts were incubated with the radiolabeled m67-SIE probe and separated on a polyacrylamide gel, and radioactivity was determined using a phosphor imaging screen. Supershifts were performed using antibodies recognizing either STAT1 $\!\alpha$ and STAT1 $\!\beta$ (lanes 3 and 9) or STAT1 α alone (lane 8). Supershifts show that the lower band (lane 7) comprises only STAT1 β homodimers, whereas the upper bands (lanes 1, 2, and 5) comprise STAT1α homodimers and STAT1α/ STAT1β heterodimers, respectively. Note that a/a, a/b, and b/b represent the 3 different complexes binding specifically to the SIE probe. NS indicates nonspecific binding; and BS, supershifted bands (lanes

specific DNA-binding activity of STAT1 α in the absence and in the presence of IFN- γ . As expected, constitutive phosphorylation of STAT1 α (P-STAT1 α) was detected in nontransfected LCL cells and untreated CKR 516 STAT1 β -transfected cells (Figure 3A, lanes 1, 3, 7). Note that STAT1 α protein levels and phosphorylation were decreased in untreated CKR 516 STAT1 β cells (compare lanes 1 and 3). Doxycycline treatment of transfected cells was associated with both a decrease in STAT1 α phosphorylation (Figure 3A, compare lanes 5 and 3 and lanes 9 and 7) and an increase in STAT1 β phosphorylation (P-STAT1 β) (Figure 3A, compare lanes 9 and 7). Treatment with IFN- γ strongly induced the phosphorylation of STAT1 α and STAT1 β in control cells (Figure 3A, lane 2), but there was a marked inversion in the ratio of phosphorylated STAT1 isoforms in doxycycline-treated CKR516-STAT1 β -transfected cells (Figure 3A, compare lanes 3 and 5 and lanes 4 and 6).

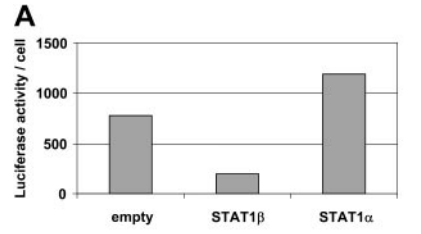
Electrophoretic mobility shift assays (EMSAs) were performed to analyze the DNA-binding activity of STAT1 α and STAT1 β . A weak constitutive binding of STAT1 complexes to the SIE probe was detected in nontransfected cells (Figure 3B, lane 1). Treatment with IFN- γ markedly increased this binding activity (lane 2). As expected, adding it to the incubation of a STAT1-specific antibody resulted in a near complete supershift of this band (Figure 3B, lane 3). In CKR516-STAT1 β -transfected cells, the constitutive binding to the SIE probe was nearly undetectable (Figure 3B, lane 4), correlating with a decrease of P-STAT1 α in these cells compared

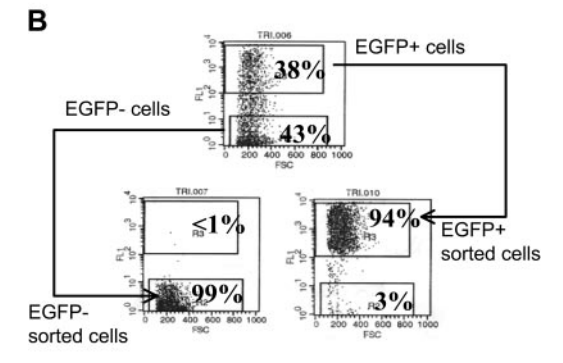
with parental cells (Figure 3A, lane 3). Treatment with IFN-y allowed observation of the binding of STAT1 complexes to the SIE probe in CKR516-STAT1β-transfected cells (Figure 3B, lane 5). No binding to the SIE probe was detected after doxycycline treatment (Figure 3B, lane 6), in agreement with Western blot analysis showing the decrease of P-STAT1α levels (Figure 3A, lanes 5 and 9). After the induction of STAT1B by doxycycline, the normally IFN-γ-induced STAT1 binding activity was decreased and a new SIE-binding activity was detected (Figure 3B, compare lanes 7 and 5). Supershifts with antibodies specific to STAT1 α alone or to STAT1 α and STAT1 β showed that this new SIE-binding activity corresponded to the STAT1ß homodimer, whereas IFN-y-induced (lanes 2, 5, 7) and constitutive SIEbinding activities (lane 1) corresponded to STAT1α homodimers and $STAT1\alpha/\beta$ heterodimers (lanes 8 and 9). Therefore, though STAT1α and STAT1β were constitutively phosphorylated in LCL cells, there was a marked excess of phospho-STAT1α. In addition, the overexpression of STAT1B was associated with decreased phosphorylation and DNA-binding activity of STAT1α. As mentioned in "Materials and methods," the slight leakiness of the vector used in this study may account for the diminished SIE binding activity observed in noninduced CKR516-STAT1βtransfected cells.

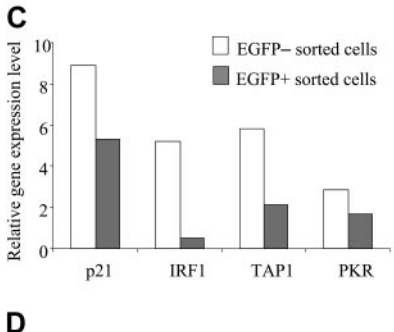
Transcriptional activity of STAT1 was determined in the CKR516-STAT1 β - or the CKR516-STAT1 α -transfected cells by cotransfecting a plasmid with luciferase as a reporter gene, driven by the TAP1 promoter in which the κB site had been mutated. Results showed that inducing STAT1B expression dramatically reduced TAP1 promoter activity (Figure 4A), confirming the inhibitory role of STAT1β. STAT1α target gene expression was then analyzed in homogeneous cell populations obtained by cell sorting highly induced EGFP/STAT1B positive and noninduced negative cells (Figure 4B). In both populations, expression of the endogenous STAT1α target genes—p21WAF1/CIP1, IRF1, PKR, TAP1—was assessed by real-time quantitative polymerase chain reaction (RQ-PCR) (Figure 4C), showing that their mRNA levels, especially those of IRF1, were decreased in sorted EGFP/STAT1β cells. Given that c-myc expression is known to be down-regulated by IFN-γ,⁴⁹ we analyzed its expression in CKR516-STAT1βtransfected cells. We found that IFN- γ treatment was associated with a decrease of c-myc protein expression and that this effect was reverted by the overexpression of STAT1B (Figure 4D). Thus, inhibiting the phosphorylation, the DNA-binding activity, and the transcriptional activity of STAT1a by STAT1B overexpression correlates with the inhibition of gene expression involved in the regulation of the cell cycle.

Overexpression of STAT1 β overcomes fludarabine-induced cell cycle arrest and apoptosis and promotes cell proliferation

To determine the effect of the induction of STAT1 β on cell proliferation and apoptosis induced by DNA damage after treatment with fludarabine for 24 hours, 2 homogeneous EGFP/STAT1 β -positive and EGFP/STAT1 β -negative cell populations were obtained by sorting. An identical experiment was performed with cells overexpressing STAT1 α . Proliferation kinetics showed a decrease of the doubling time of EGFP/STAT1 β -positive sorted cells compared with their EGFP/STAT1 β -negative counterparts (Figure 5A). The number of cells in S phase, as measured by BrdU incorporation and flow cytometry, was similar in EGFP/STAT1 β -(Figure 5B) and EGFP/STAT1 α -expressing cells (Figure 5C) compared with noninduced cells. Adding fludarabine resulted in







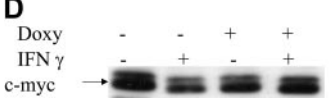


Figure 4. Down-regulation of STAT1 α target genes in STAT1 β overexpressing cells. (A) Inhibition of the transcriptional activity of STAT1 a by overexpression of $\text{STAT1}\beta.$ Cells were cotransfected with a plasmid construct containing the luciferase gene driven by the TAP1 promoter with an inactivated kB site. Cells were transfected with an empty CKR516 vector (empty), with the CKR516-STAT1 β vector, or with the CKRSTAT1 α vector. The experiment was repeated 3 times with identical results. (B) Purification of EGFP-inducible and noninducible cells transfected with the CKR516-STAT1 β vector. Twenty-four hours of treatment of cells with 0.6 μ g/mL doxycycline yielded a heterogeneous cell population (top graph) containing EGFP-positive (top gate) and -negative cells (bottom gate). A typical result of EGFP-positive and -negative cell sorting by flow cytometry is shown in the bottom graphs. The percentage of cells in the 2 gates is indicated in each graph. (C) RQ-PCR analysis of STAT1 target genes in CKR516-STAT1\(\beta\)-transfected cells. Levels of p21WAF1/ CIP1, IRF1, PKR, and TAP1 mRNA were measured by RQ-PCR in extracts from EGFP-positive and -negative sorted cells and compared to the level of Abl1 mRNA. (D) Detection of the c-myc protein in CKR516-STAT1β-transfected cells. Detection of c-myc was performed by Western blot analysis of total protein extracts from cells treated (+) or not treated (-) with 0.6 µg/mL doxycycline for 24 hours.

cell cycle arrest in noninduced cells transfected with the STAT1 β or STAT1 α expression vector. Overexpression of STAT1 β markedly overcame fludarabine-induced cell cycle arrest. This was specific to STAT1 β overexpression because the cell cycle arrest induced by fludarabine was not affected by the overexpression of STAT1 α (Figure 5B-C).

The rate of spontaneous apoptosis was decreased in sorted EGFP/STAT1 β -positive cells compared with EGFP/STAT1 β -negative cells (Figure 6A). Moreover, the overexpression of STAT1 β markedly reduced fludarabine-induced apoptosis (Figure 6A; in induced cells, apoptotic cells in the sub- G_1 peak were down

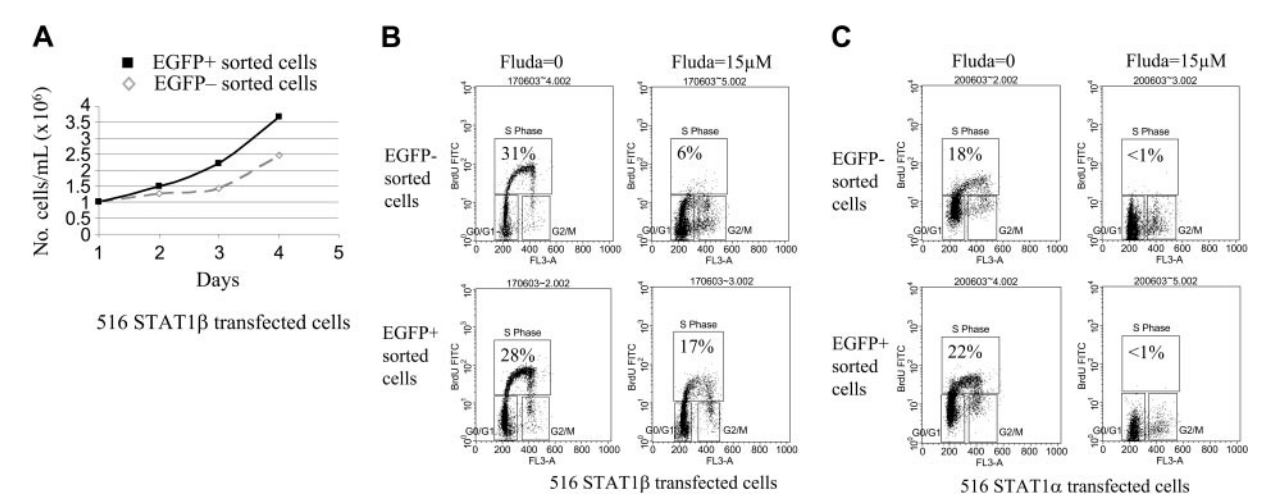


Figure 5. Cell cycle analysis of CKR516-STAT1 β – and CKR516-STAT1 α –transfected cells treated or not treated with fludarabine. EGFP-positive and -negative cells were sorted by fluorescence-activated cell sorting (FACS) as for Figure 4A, after treatment of the cells with 0.6 μg/mL doxycycline for 24 hours. (A) Difference in proliferation rates of the EGFP-positive and -negative purified cells from CKR516-STAT1 β –transfected cells. The 2 cell populations were grown in the presence (\blacksquare) or absence (\Diamond) of doxycycline over 4 days and were counted each day. The experiment was repeated twice. (B) Resistance to fludarabine-induced inhibition of cell proliferation in CKR516-STAT1 β –transfected cells. EGFP-positive and -negative cell populations were purified by FACS after doxycycline treatment and were further treated or not treated with 15 μM fludarabine for 16 hours. The cell cycle was analyzed by flow cytometry after BrdU incorporation. The percentage of cells in the S phase is indicated within each diagram. (C) Absence of resistance to fludarabine-induced inhibition of cell proliferation in CKR516-STAT1 α –transfected cells. As for panel B, the EGFP-positive and -negative cell populations purified by FACS were further treated with 15 μM fludarabine or left untreated. The percentage of cells in the S phase is indicated within each diagram. Results are representative of at least 2 independent experiments.

to 9.4% instead of 29.5%). This result was confirmed by the analysis of cleaved PARP using Western blotting (note the reduced PARP cleavage in Figure 6B, lanes 3 and 4 compared with lanes 1 and 2). Thus, STAT1 β overexpression leads to resistance to fludarabine-induced apoptosis, an indication that DNA damage—induced apoptosis and cell cycle arrest are dependent on STAT1 α activity.

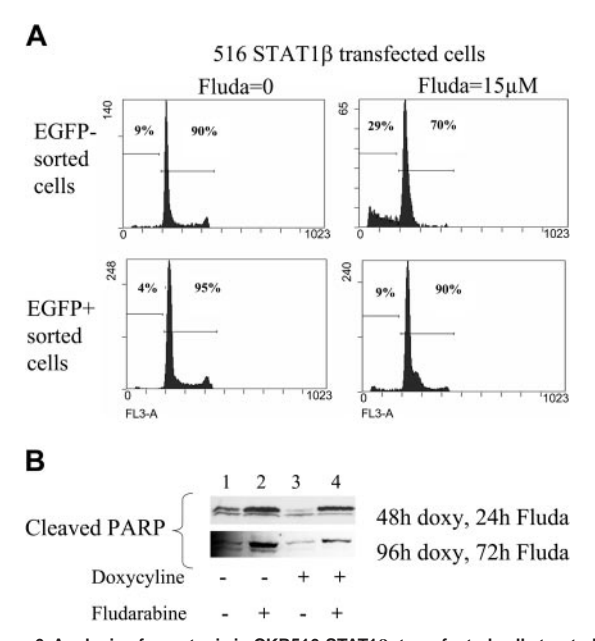


Figure 6. Analysis of apoptosis in CKR516-STAT1β–transfected cells treated or not treated with fludarabine. (A) Analysis of the sub- G_1 peak. EGFP-positive and -negative cell populations purified by FACS after doxycycline treatment were further treated with 15 μM fludarabine for 16 hours or were left untreated. DNA content was assessed by flow cytometry using the 7AAD dye after ethanol fixation, allowing quantification of the sub- G_1 peak. (B) Analysis of PARP cleavage. Detection of the PARP fragment cleaved by caspase 3 was performed by Western blotting of total protein extracts from cells treated (+) or not treated (–) with 0.6 μg/mL doxycycline for 24 hours and treated (+) or not treated (–) with fludarabine for 24 and 72 hours. Results are representative of at least 2 independent experiments.

STAT1 α down-regulates Mdm2 expression and is physically associated with p53

The inhibition of STAT1α by STAT1β led to fludarabine-induced apoptosis resistance. On the other hand, DNA damage-induced apoptosis was p53 dependent, and the stability of p53 was regulated by Mdm2.⁵⁰ To investigate the role of STAT1 in the p53 apoptosis pathway, STAT1B was overexpressed, cells were either treated or not treated with IFN-y or with fludarabine for 24 hours, and the mRNA levels of Mdm2 and p53 were assessed using RQ-PCR. The p53 mRNA levels were not significantly different in cells that were treated or not treated with IFN-y or fludarabine (Figure 7A). Conversely, Mdm2 mRNA levels were regulated by STAT1. The mere overexpression of STAT1β had no effect on the expression of Mdm2 mRNA, but when cells were treated with IFN- γ , the expression of Mdm2 decreased, and this was abolished by the overexpression of STAT1\(\beta\). In cells treated with fludarabine, the expression of Mdm2 was strongly diminished, but when STAT1B was overexpressed, this negative regulation was significantly reduced (Figure 7A). These results, summarized in Figure 7B in which the ratios of p53 and Mdm2 mRNA were calculated, showed that treatment with fludarabine and, to a lesser extent, with IFN-γ increased the p53/Mdm2 mRNA ratio, and they also showed that this increase is counteracted by STAT1B. Thus, regulating the expression of Mdm2 by STAT1α indicated that it participated in the stability of p53, thus explaining why part of the effect of fludarabine requires STAT1 activity.

To further document the involvement of STAT1 α activity in DNA damage–induced apoptosis, we analyzed the subcellular location of p53 by immunofluorescence staining. We observed that the nuclear localization of p53 induced by fludarabine was prevented by the overexpression of STAT1 β (Figure 7C, lower panels). In STAT1 α overexpressing cells, not only was the nuclear localization of p53 induced by fludarabine not inhibited, it was enhanced when compared with EGFP-negative cells (Figure 7C, upper panels). Finally, to detect the possible association of

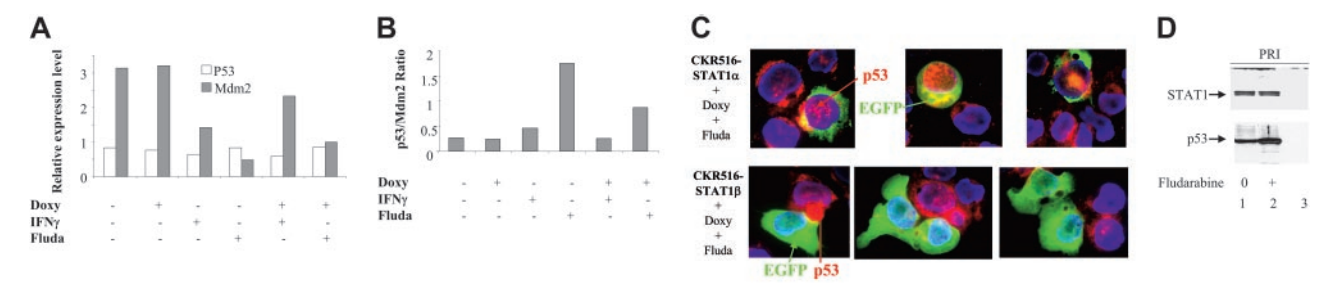


Figure 7. Regulation of p53 and Mdm2 mRNA expression by STAT1 α and p53/STAT1 α proapoptotic complex. (A) Determination by RQ-PCR of the relative expression levels of p53 and Mdm2 in EGFP-positive and -negative cells from CKR516-STAT1 β -transfected cells. Induced (+) and noninduced (-) cells were treated with doxycycline (Doxy), IFN- γ (250 U/mL), or 15 μM fludarabine for 16 hours. Relative mRNA expression levels were assessed by RQ-PCR using Abl1 mRNA and a pool of RNA for normalization. Results are representative of at least 2 independent experiments. (B) p53/Mdm2 ratios of mRNA measured by RQ-PCR in EGFP-positive and -negative cells from CKR516-STAT1 β -transfected cells. p53/Mdm2 mRNA ratios were calculated from the experiment described for panel A. Results are representative of at least 2 independent experiments. (C) Detection of p53 by immunofluorescence staining in EGFP-positive cells from CKR516-STAT1 β —and STAT1 α —transfected cells. Cells were transfected with CKR516-STAT1 α (top panels) or CKR516-STAT1 β (bottom panels), pretreated with doxycycline for 24 hours (inducibility reached 70%), and treated with fludarabine for 24 hours. Cytospins were stained with AlexaFluor 594 streptavidin for the detection of the secondary biotinylated immune serum against the p53 antibody (red) and with DAPI (blue) for nucleus staining. Induced cells are recognized by the presence of EGFP (green) in the cytoplasm. In CKR516-STAT1 α EGFP-positive cells, high levels of p53 (red) were localized in the nucleus when compared with EGFP-negative cells. Conversely, in CKR516-STAT1 β EGFP-positive cells, no p53 was visible in the nucleus, similar to noninduced cells. (D) Physical association of STAT1 α to p53 bound to the p53 DNA-specific probe. Nuclear extracts were obtained from nontransfected (PRI) cells treated (+) or not (-) with fludarabine. Extracts were incubated with biotinylated p53 DNA-specific probe. Complexes were captured on agarose—streptavidin, then washed and separated by electrophoresis. Western bl

activated p53 and STAT1 α , we performed a pull-down assay with a biotinylated oligonucleotide containing the consensus p53 binding sequence. Detecting the proteins bound to the oligonucleotide by Western blotting showed that STAT1 α and p53 were physically associated (Figure 7D), suggesting that the interaction of p53 and STAT1 α is an important aspect of the cellular response to DNA damage.

Discussion

The aim of this study was to analyze the roles of STAT1 α and STAT1 β in DNA damage–induced apoptosis and cell cycle arrest in B cells in response to fludarabine treatment. To this end, we used EBV-immortalized lymphoblastoid cell lines in which STAT1 is constitutively activated.³⁹

We used an episomal tetracycline-based inducible system 40 to overexpress STAT1 β , a naturally occurring dominant-negative inhibitor of STAT1 α . To measure the induction rate, we used a vector that coexpresses STAT1 β and EGFP as a marker of induction, driven by a bidirectional tetracycline promoter. The induction of EGFP was clearly dependent on the concentration of doxycycline, and the inductions of EGFP and STAT1 β were tightly correlated. This experimental system has 2 great advantages. First, it allows monitoring of the level of induction, an important parameter for the interpretation of the results obtained. Second, it allows the separation of induced from noninduced cells through cell sorting. Because induced and noninduced cells are subjected to strictly identical conditions, the control is always included within the experiment.

It was previously hypothesized that STAT1 β binds to the same DNA sequences as STAT1 α without being able to transactivate genes.^{4,51} Binding of STAT1 β to the STAT1 α DNA targets was confirmed in vitro,⁵² and it was demonstrated that STAT1 β , and mutated forms of STAT1 α , act as dominant-negative inhibitors of STAT1 α . Our EMSA results showed that STAT1 β overexpression is associated with a dramatic decrease in the DNA-binding activity of STAT1 α . The inhibition by STAT1 β of the activation of STAT1 α may occur at different levels within the cell. In this study, STAT1 β

overexpression inhibited the phosphorylation of STAT1 α , but it was associated with an elevation of its own phosphorylation. Thus, STAT1 β may interfere with the activation of STAT1 α by saturation of its binding sites at the receptor level, thereby confirming the constitutive activation of the signal transduction pathway leading to STAT1 phosphorylation in LCLs. In addition, STAT1 β may also inhibit STAT1 α by occupying its DNA-binding sequences in the nucleus, thus inhibiting transcription of the STAT1 α target genes.

Our experiments further demonstrate that the overexpression of STAT1 β , which blocked the phosphorylation of STAT1 α , its specific binding to DNA, also blocked the induction of endogenous cellular STAT1 α target genes such as *TAP1*, *IRF1*, *PKR*, and *p21WAF1/CIP1*. Conversely, the decreased c-myc expression known to result from the stimulation of STAT1 α by IFN- γ was reverted by the overexpression of STAT1 β .

STAT1 may have a tumor-suppressor function that inhibits cell growth and apoptosis. This function could be triggered by fludarabine, which is otherwise known to induce apoptosis and cell cycle arrest through activation of p53. Indeed, p53 and STAT1 modulate similar target genes, notably *p21WAF1*.⁶

Along this line, our results clearly showed that inhibiting STAT1α protects the cells against fludarabine-induced apoptosis, indicating that although resistance to fludarabine was observed in EBV-infected cells expressing high levels of STAT1, this resistance did not result from STAT1 activation, as previously suggested.^{29,30} STAT1B protects cells against apoptosis and favors cell proliferation, whereas STAT1 α participates in the negative regulation of cell proliferation. Cell proliferation is reduced in EBV-infected (socalled converted BL cell lines) and LMP1-transfected Burkitt lymphoma cell lines compared with their EBV-negative counterparts. 53-55 This decrease in cell proliferation correlates with the constitutive activation of STAT1 α in these cells regardless of the EBV-induced decrease of p53 expression. The involvement of STAT1α may be linked in part to the induction of cell cycle inhibitor p21WAF1/ CIP1 expression^{6,56} and to the suppression of c-myc expression because of binding to the IFN gamma activation site (GAS) element in the c-myc promoter, 49 presumably through interaction with a corepressor.

Regarding the response to DNA damage, our results, in accordance with those found in human fibrosarcoma cell lines, 32 indicate that STAT1 β is necessary for DNA damage-induced cell cycle arrest and apoptosis in human B cells. Given that inducing cell cycle arrest and apoptosis by fludarabine is clearly ascribed to the function of p53, our data imply that STAT1 β is a cofactor for p53 in this system. STAT1 α may promote apoptosis by 2 synergetic ways: it negatively regulates the expression of Mdm2, the major factor that controls p53 degradation, and it associates with p53 and modulates its activity. This poses the STAT1 activation pathway, and particularly the STAT1 α /STAT1 β balance, as a potential new therapeutic target that could overcome, for instance, the resistance of cells to fludarabine-induced apoptosis.

Acknowledgments

We thank J. Darnell (Rockefeller University, New York, NY) for providing the DNA clones encoding STAT1 α and STAT1 β and to D. Johnson (National Institutes of Health, Bethesda, MD) for providing the TAP1/luciferase reporter plasmid. We thank C. Jaillat (UMR INRA 1061, Université de Limoges, France), and J.L. Faucher, A. Allegreaud, and A. Carassus (Laboratoire d'Hématologie, CHU Dupuytren, Limoges, France) for assistance in cell sorting, cell cycle analysis, cell culture and immunofluorescence, respectively. We thank I. Youlyouz and N. Cogné for helpful assistance in plasmid constructs and real-time quantitative PCR.

References

- Fu XY, Kessler DS, Veals SA, Levy DE, Darnell JE Jr. ISGF3, the transcriptional activator induced by interferon alpha, consists of multiple interacting polypeptide chains. Proc Natl Acad Sci U S A. 1990;87:8555-8559.
- Kessler DS, Veals SA, Fu XY, Levy DE. Interferon-alpha regulates nuclear translocation and DNA-binding affinity of ISGF3, a multimeric transcriptional activator. Genes Dev. 1990;4:1753-1765
- Schindler C. Cytokine signal transduction. Receptor. 1995;5:51-62.
- Shuai K, Schindler C, Prezioso VR, Darnell JE Jr. Activation of transcription by IFN-gamma: tyrosine phosphorylation of a 91-kD DNA binding protein. Science. 1992;258:1808-1812.
- Bromberg JF, Horvath CM, Wen Z, Schreiber RD, Darnell JE Jr. Transcriptionally active Stat1 is required for the antiproliferative effects of both interferon alpha and interferon gamma. Proc Natl Acad Sci U S A. 1996;93:7673-7678.
- Chin YE, Kitagawa M, Su WC, You ZH, Iwamoto Y, Fu XY. Cell growth arrest and induction of cyclin-dependent kinase inhibitor p21 WAF1/CIP1 mediated by STAT1. Science. 1996;272:719-722
- Chin YE, Kitagawa M, Kuida K, Flavell RA, Fu XY. Activation of the STAT signaling pathway can cause expression of caspase 1 and apoptosis. Mol Cell Biol. 1997;17:5328-5337.
- Garcia-Sastre A, Durbin RK, Zheng H, et al. The role of interferon in influenza virus tissue tropism. J Virol. 1998;72:8550-8558.
- Hoey T, Schindler U. STAT structure and function in signaling. Curr Opin Genet Dev. 1998;8:582-597.
- Kaplan MH, Grusby MJ. Regulation of T helper cell differentiation by STAT molecules. J Leukoc Biol. 1998:64:2-5.
- Kumar A, Commane M, Flickinger TW, Horvath CM, Stark GR. Defective TNF-alpha-induced apoptosis in STAT1-null cells due to low constitutive levels of caspases. Science. 1997;278:1630-1632.
- Leonard WJ. Role of Jak kinases and STATs in cytokine signal transduction. Int J Hematol. 2001; 73:271-277.
- Su WC, Kitagawa M, Xue N, et al. Activation of Stat1 by mutant fibroblast growth-factor receptor in thanatophoric dysplasia type II dwarfism. Nature. 1997;386:288-292.
- 14. Darnell JE Jr. STATs and gene regulation. Science. 1997;277:1630-1635.
- Pranada AL, Metz S, Herrmann A, Heinrich PC, Muller-Newen G. Real Time analysis of STAT3 nucleocytoplasmic shuttling. J Biol Chem. 2004; 279:15114-15123.
- Muller M, Laxton C, Briscoe J, et al. Complementation of a mutant cell line: central role of the 91 kDa polypeptide of ISGF3 in the interferon-alpha

- and -gamma signal transduction pathways. EMBO J. 1993:12:4221-4228.
- Shen Y, Darnell JE Jr. Antiviral response in cells containing Stat1 with heterologous transactivation domains. J Virol. 2001;75:2627-2633.
- Wen Z, Zhong Z, Darnell JE Jr. Maximal activation of transcription by Stat1 and Stat3 requires both tyrosine and serine phosphorylation. Cell. 1995;82:241-250
- Wen Z, Darnell JE Jr. Mapping of Stat3 serine phosphorylation to a single residue (727) and evidence that serine phosphorylation has no influence on DNA binding of Stat1 and Stat3. Nucleic Acids Res. 1997;25:2062-2067.
- Schindler C, Fu XY, Improta T, Aebersold R, Darnell JE Jr. Proteins of transcription factor ISGF-3: one gene encodes the 91- and 84-kDa ISGF-3 proteins that are activated by interferon alpha. Proc Natl Acad Sci U S A. 1992;89:7836-7839.
- Miller WE, Mosialos G, Kieff E, Raab-Traub N. Epstein-Barr virus LMP1 induction of the epidermal growth factor receptor is mediated through a TRAF signaling pathway distinct from NF-kappaB activation. J Virol. 1997;71:586-594.
- Walter MJ, Look DC, Tidwell RM, Roswit WT, Holtzman MJ. Targeted inhibition of interferongamma—dependent intercellular adhesion molecule-1 (ICAM-1) expression using dominantnegative Stat1. J Biol Chem. 1997;272:28582-28589.
- Bromberg JF, Fan Z, Brown C, Mendelsohn J, Darnell JE Jr. Epidermal growth factor-induced growth inhibition requires Stat1 activation. Cell Growth Differ. 1998;9:505-512.
- Taniguchi T. Transcription factors IRF-1 and IRF-2: linking the immune responses and tumor suppression. J Cell Physiol. 1997;173:128-130.
- Kanda K, Kempkes B, Bornkamm GW, von Gabain A, Decker T. The Epstein-Barr virus nuclear antigen 2 (EBNA2), a protein required for B lymphocyte immortalization, induces the synthesis of type I interferon in Burkitt's lymphoma cell lines. Biol Chem. 1999;380:213-221.
- Lee KY, Anderson E, Madani K, Rosen GD. Loss of STAT1 expression confers resistance to IFNgamma-induced apoptosis in ME180 cells. FEBS Lett. 1999;459:323-326.
- Asao H, Fu XY. Interferon-gamma has dual potentials in inhibiting or promoting cell proliferation J Biol Chem. 2000;275:867-874.
- Gandhi V, Plunkett W. Cellular and clinical pharmacology of fludarabine. Clin Pharmacokinet. 2002;41:93-103.
- Frank DA, Mahajan S, Ritz J. Fludarabine-induced immunosuppression is associated with inhibition of STAT1 signaling. Nat Med. 1999;5: 444-447.
- 30. Fagard R, Mouas H, Dusanter-Fourt I, et al. Resistance to fludarabine-induced apoptosis in Ep-

- stein-Barr virus infected B cells. Oncogene. 2002; 21:4473-4480.
- Vallat L, Magdelenat H, Merle-Beral H, et al. The resistance of B-CLL cells to DNA damage-induced apoptosis defined by DNA microarrays. Blood. 2003;101:4598-4606.
- Townsend PA, Scarabelli TM, Davidson SM, Knight RA, Latchman DS, Stephanou A. STAT-1 interacts with p53 to enhance DNA damage-induced apoptosis. J Biol Chem. 2004;279:5811-5820.
- Wang Y, Wu TR, Cai S, Welte T, Chin YE. Stat1
 as a component of tumor necrosis factor α receptor 1-TRADD signaling complex to inhibit NF-κB
 activation. Mol Cell Biol. 2000;20:4505-4512.
- McLaughlin P, Hagemeister FB, Rodriguez MA, et al. Safety of fludarabine, mitoxantrone, and dexamethasone combined with rituximab in the treatment of stage IV indolent lymphoma. Semin Oncol. 2000;27:37-41.
- Tsimberidou AM, McLaughlin P, Younes A, et al. Fludarabine, mitoxantrone, dexamethasone (FND) compared with an alternating triple therapy (ATT) regimen in patients with stage IV indolent lymphoma. Blood. 2002;100:4351-4357.
- Lynch JW, Hei DL, Braylan RC, et al. Phase II study of fludarabine combined with interferonalpha-2a followed by maintenance therapy with interferon-alpha-2a in patients with low-grade non-Hodgkin's lymphoma. Am J Clin Oncol. 2002; 25:391-397.
- Wilder DD, Ogden JL, Jain VK. Efficacy of fludarabine/mitoxantrone/dexamethasone alternating with CHOP in bulky follicular non-Hodgkin's lymphoma. Clin Lymphoma. 2002;2:229-237.
- Mauro FR, Zinzani P, Zaja F, et al. Fludarabine + prednisone alpha-interferon followed or not by alpha-interferon maintenance therapy for previously untreated patients with chronic lymphocytic leukemia: long term results of a randomized study. Haematologica. 2003;88:1348-1357.
- Weber-Nordt RM, Egen C, Wehinger J, et al. Constitutive activation of STAT proteins in primary lymphoid and myeloid leukemia cells and in Epstein-Barr virus (EBV)–related lymphoma cell lines. Blood. 1996;88:809-816.
- Feuillard J, Schuhmacher M, Kohanna S, et al. Inducible loss of NF-xB activity is associated with apoptosis and Bcl-2 down-regulation in Epstein-Barr virus-transformed B lymphocytes. Blood. 2000;95:2068-2075.
- Urlinger S, Baron U, Thellmann M, Hasan MT, Bujard H, Hillen W. Exploring the sequence space for tetracycline-dependent transcriptional activators: novel mutations yield expanded range and sensitivity. Proc Natl Acad Sci U S A. 2000; 97:7963-7968.
- Annweiler A, Muller U, Wirth T. Functional analysis of defined mutations in the immunoglobulin heavy-chain enhancer in transgenic mice. Nucleic Acids Res. 1992;20:1503-1509.

- Baron U, Gossen M, Bujard H. Tetracycline-controlled transcription in eukaryotes: novel transactivators with graded transactivation potential. Nucleic Acids Res. 1997;25:2723-2729.
- Baron U, Bujard H. Tet repressor-based system for regulated gene expression in eukaryotic cells: principles and advances. Methods Enzymol. 2000;327:401-421.
- Zhang X, Blenis J, Li HC, Schindler C, Chen-Kiang S. Requirement of serine phosphorylation for formation of STAT-promoter complexes. Science. 1995;267:1990-1994.
- Feuillard J, Gouy H, Bismuth G, Lee LM, Debre P, Korner M. NF-kappa B activation by tumor necrosis factor alpha in the Jurkat T cell line is independent of protein kinase A, protein kinase C, and Ca(2+)-regulated kinases. Cytokine. 1991;3:257-265
- 47. Gabert J, Beillard E, van der Velden VH, et al. Standardization and quality control studies of "real-time" quantitative reverse transcriptase polymerase chain reaction of fusion gene transcripts for residual disease detection in leuke-

- mia—a Europe Against Cancer program. Leukemia. 2003;17:2318-2357.
- Baron U, Freundlieb S, Gossen M, Bujard H. Coregulation of two gene activities by tetracycline via a bidirectional promoter. Nucleic Acids Res. 1995;23:3605-3606.
- Ramana CV, Grammatikakis N, Chernov M, et al. Regulation of c-myc expression by IFN-gamma through Stat1-dependent and -independent pathways. EMBO J. 2000;19:263-272.
- Chen L, Agrawal S, Zhou W, Zhang R, Chen J. Synergistic activation of p53 by inhibition of MDM2 expression and DNA damage. Proc Natl Acad Sci U S A. 1998;95:195-200.
- Shuai K, Stark GR, Kerr IM, Darnell JE Jr. A single phosphotyrosine residue of Stat91 required for gene activation by interferon-gamma. Science. 1993;261:1744-1746.
- Vinkemeier U, Cohen SL, Moarefi I, Chait BT, Kuriyan J, Darnell JE Jr. DNA binding of in vitro activated Stat1 alpha, Stat1 beta and truncated Stat1: interaction between NH2-terminal domains

stabilizes binding of two dimers to tandem DNA sites. EMBO J. 1996;15:5616-5626.

2483

- Baran-Marszak F, Fagard R, Girard B, et al. Gene array identification of Epstein Barr virus-regulated cellular genes in EBV-converted Burkitt lymphoma cell lines. Lab Invest. 2002;82:1463-1479.
- Cuomo L, Ramquist T, Trivedi P, Wang F, Klein G, Masucci MG. Expression of the Epstein-Barr virus (EBV)-encoded membrane protein LMP1 impairs the in vitro growth, clonability and tumorigenicity of an EBV-negative Burkitt lymphoma line. Int J Cancer. 1992:51:949-955.
- Torsteinsdottir S, Andersson ML, Avila-Carino J, et al. Reversion of tumorigenicity and decreased agarose clonability after EBV conversion of an IgH/myc translocation–carrying BL line. Int J Cancer. 1989;43:273-278.
- Kominsky S, Johnson HM, Bryan G, et al. IFN-γ inhibition of cell growth in glioblastomas correlates with increased levels of the cyclin dependent kinase inhibitor p21WAF1/CIP1. Oncogene. 1998;17:2973-2979.



2004 104: 2475-2483 doi:10.1182/blood-2003-10-3508 originally published online June 24, 2004

Differential roles of STAT1 α and STAT1 β in fludarabine-induced cell cycle arrest and apoptosis in human B cells

Fanny Baran-Marszak, Jean Feuillard, Imen Najjar, Christophe Le Clorennec, Jean-Marie Béchet, Isabelle Dusanter-Fourt, Georg W. Bornkamm, Martine Raphaël and Remi Fagard

Updated information and services can be found at: http://www.bloodjournal.org/content/104/8/2475.full.html

Articles on similar topics can be found in the following Blood collections Apoptosis (746 articles) Cell Adhesion and Motility (790 articles) Immunobiology (5391 articles) Neoplasia (4182 articles) Signal Transduction (1930 articles)

Information about reproducing this article in parts or in its entirety may be found online at: http://www.bloodjournal.org/site/misc/rights.xhtml#repub_requests

Information about ordering reprints may be found online at: http://www.bloodjournal.org/site/misc/rights.xhtml#reprints

Information about subscriptions and ASH membership may be found online at: http://www.bloodjournal.org/site/subscriptions/index.xhtml